Magnetic recording stability of taenite-containing meteorites

Geophysical Research Letters

RESEARCH LETTER
10.1029/2022GL102602

Magnetic Recording Stability of Taenite-Containing Meteorites

José A. P. M. Devienne[1], Thomas A. Berndt[1], Wyn Williams[2], and Lesleis Nagy[3]

[1]Department of Geophysics, School of Earth and Space Sciences, Peking University, Beijing, PR China, [2]School of GeoSciences, The University of Edinburgh, Edinburgh, UK, [3]Department of Geophysics, Ocean and Ecological Sciences, University of Liverpool, Liverpool, UK

Key Points:

- Nanometer-scaled taenite observed in different meteoritic microstructures are magnetically stable over billion-years timescales
- Taenite-containing cloudy zones are dominates by uniform states able to record stable magnetizations as grains grow through ~14 nm
- Vortex states observed in larger (>50 nm) taenite grains are also highly stable, but may be reset upon tetrataenite ordering

Supporting Information:

Supporting Information may be found in the online version of this article.

Correspondence to:

J. A. P. M. Devienne,
devienne@stu.pku.edu.cn

Citation:

Devienne, J. A. P. M., Berndt, T. A., Williams, W., & Nagy, L. (2023). Magnetic recording stability of taenite-containing meteorites. *Geophysical Research Letters*, *50*, e2022GL102602. https://doi.org/10.1029/2022GL102602

Received 19 JAN 2023
Accepted 13 JUN 2023

Abstract Sub-μm taenite and tetrataenite grains observed in a number of (stony-)iron meteorite groups are promising sources of paleomagnetic records in meteorites. While slowly-cooled meteorites form tetrataenite—an extremely good recorder—, fast-cooled meteorites may contain fine-grained taenite, which was considered unsuitable for paleomagnetic studies. In this work, however, we show that nm-sized taenite grains are stable over billion-year timescales, indicating that taenite-bearing meteorites are reliable sources of paleomagnetic information. We find a range of sizes for which taenite forms stable single-domain structures, which coincides with the grain sizes observed in the cloudy zone of most fast cooled IVA meteorites. These meteorites, therefore, can provide reliable paleomagnetic information recorded as a stable crystallization remanent magnetization as taenite grains grown. Vortex states observed in larger (>50 nm) grain sizes are also highly stable, indicating that coarse-grained taenite observed in meteoritic microstructures can also provide reliable records of paleomagnetic fields.

Plain Language Summary Metallic meteorites are fragments of small planetary bodies that formed during the first million years of our solar system. They can provide a wealth of information about how small planets form, how they undergo differentiation and whether (and how) they once had a liquid core capable of generating self-driven magnetic fields. Recent works have shown that nanometer-sized tetrataenite grains present in slowly cooled meteorites are able to preserve records of ancient magnetic activity of their parent bodies. In this work we show that taenite, a magnetic mineral commonly observed a number of distinct meteoritic microstructures, is also capable of reliably preserving records of ancient magnetic fields. These results open a window of opportunity in using metallic meteorites, in particular the so-called fast cooled meteorites, in understanding key aspect of planetary formation and evolution based on their magnetic records preserved in nm-sized taenite grains.

1. Introduction

Most meteorites originate from small planetary bodies (<500 km radius) formed within the first million years (Myr) of the solar system (Wright & Grady, 2006). The existence of iron and stony-iron meteorites indicates that part of these bodies underwent large-scale differentiation (Elkins-Tanton et al., 2011; McCoy et al., 2006), possibly generating planetary magnetic fields by dynamo processes due to convection of molten metallic cores (Bryson et al., 2015; Nichols et al., 2016). Recent paleomagnetic studies in (stony-)iron meteorites suggest that these materials can preserve magnetic records of planetary fields generated by their parent bodies (Maurel et al., 2020; Nichols et al., 2016, 2021). Extracting paleomagnetic records from early solar materials is contingent on the presence of magnetic minerals capable of preserving magnetization states over solar system timescales. Taenite and tetrataenite are ferromagnetic minerals commonly observed in (stony-)iron meteorite groups—for example, IIEs (Maurel et al., 2020), IVAs (Bryson et al., 2017), IVBs (J. Yang et al., 2010), IABs (Bryson, Herrero-Albillos, et al., 2014), main group pallasite (Nichols et al., 2016)—and in ordinary chondrites (Bryson et al., 2019) that can possibly provide reliable record of ancient magnetic activity in extraterrestrial bodies (Bryson, Church, et al., 2014; Einsle et al., 2018; Mansbach et al., 2022). Mostly motivated by the exceptional recording properties of tetrataenite, much effort has been put to understand how tetrataenite-bearing meteorites records magnetizations (Bryson, Herrero-Albillos, et al., 2014; Bryson, Church, et al., 2014; Mansbach et al., 2022; Maurel et al., 2020). It remains poorly known, however, how individual taenite grains behave magnetically, that is, whether they can carry reliable paleomagnetic record over solar system timescales. Assessing which domain states form in sub-μm- to nm-scaled taenite, as well as their ability to preserve magnetization states over geological timescales,

is key for constraining the mechanisms by which taenite-dominated meteoritic microstructures records paleomagnetic fields in (stony-)iron meteorites.

Tetrataenite forms through slow cooling (cooling rates $\lesssim$150–2500°C/Myr, Nichols et al. (2020)) of meteoritic metal via chemical ordering of disordered taenite (Lewis et al., 2014). Both the degree of tetrataenite ordering as well as its grain coarsening are dependent on the cooling rate (and Ni content) of meteoritic material. Meteoritic cloudy zones (CZs) form nm-sized taenite crystals (or island) between ~400° and ~350°C (Maurel et al., 2020) that, under considerably slow cooling rates, transform into tetrataenite. In fast cooled iron meteorites (e.g., IVAs and IVBs), believed to be fragment of mantle-stripped cores exposed (J. Yang et al., 2010) to unusually rapid cooling (>150°–2500°C/Myr), the fast cooling both prevented tetrataenite ordering as well as the islands to grow bigger. CZs in fast cooled IVAs and IVBs are, therefore, expected to be dominated by fine-grained (<50 nm), disordered (or partially disordered) taenite islands. Coarse (>200 nm up to ~10 μm) taenite grains are observed in meteoritic plessite, a microstructure found almost ubiquitously in iron meteorite groups (Buchwald, 1975), and commonly in ordinary chondrites (Goldstein & Michael, 2006). Individual sub-μm taenite grains are also observed embedded in silicate in primitive achondrite (Mansbach et al., 2022). Contrarily to tetrataenite, taenite is usually considered a poor paleomagnetic recorder, mainly due to the low coercivity observed in bulk (μm to cm scale) measurements (Wasilewski, 1988). It is not known, however, if such low resistance to remagnetization observed in bulk scales can be extended to sub-μm- to nm-scaled microstructures as those found in most meteorites. Assessing the magnetic stability of sub-μm to nm-sized taenite has a pivotal importance in extracting reliable paleomagnetic information from meteorites—especially from those that underwent faster cooling—, as well as in extending the range of meteorites that can be explored paleomagnetically. To address this question, in this work we assess the magnetic recording fidelity of fast cooled, taenite-bearing iron meteorites by carrying out extensive and systematic finite-element micromagnetic simulations of taenite islands of various sizes and elongations. We show that there is a wide range of grain sizes for which taenite forms stable domain states over billion-year timescales, which indicates that taenite-containing meteoritic microstructures can provide reliable records of ancient fields experienced by early solar materials.

2. Methods

2.1. Grains Morphology

Einsle et al. (2018) used a combination of different experimental methods to characterize the morphology of the CZ islands of the Tazewell IAB sLH iron meteorite. The results indicate the predominance of prolate triaxial grains, with elongation varying between 0% and 50% for both the intermediate (island sizes between ~60 and ~120 nm) and fine ($\lesssim$50 nm) regions of the CZ. In meteoritic plessite, which forms from the decomposition of mantensite into individual taenite/tetratenite exsolutions embedded in Fe-rich kamacite matrix, grain sizes range from a few hundred nm to up to ~10 μm (Goldstein & Michael, 2006). These, in turn, are larger grains sizes than are reported in the literature for the CZs of fast cooled iron meteorites, in which the island sizes range from ~12 to ~32 nm (Table S4 in Supporting Information S1). In this work we used finite-element micromagnetic modeling to investigate the magnetic stability of nm-sized taenite with sizes varying between 10 and 90 nm (in equivalent spherical volume diameter), considering two different grain geometries: (a) prolate spheroids and (b) triaxial ellipsoids (Figure 1). For both geometries the elongation is set along the [001] (easy-)direction of the cubic crystal structure of taenite. Percentage elongations varying between 0% and 50% are considered, such that 0% correspond to an equidimensional shape (in this study, a sphere) and 50% correspond to a short to long axis ratio (e) equal to 0.5. Triaxial particles have an intermediate axis 5% longer than the short axis (Figure 1b).

2.2. Micromagnetic Modeling

The finite-element micromagnetic modeling package MERRILL (Ó Conbhuí et al., 2018) (version 1.5.2) is used to execute the simulations. For taenite, the room-temperature magnetic parameters used in this work are: saturation magnetization M_s = 1,273 kA/m, anisotropy constant K_1 = 1 kJ/m^3 and exchange constant $A = 1.13 \times 10^{-11}$ J/m (Gehrmann, 2005; Hÿtch et al., 2003). The meshed volumes describing the grains morphology are created using the software Coreform Cubit (version 2021.11). The resolution of the mesh of the particle is constrained to be

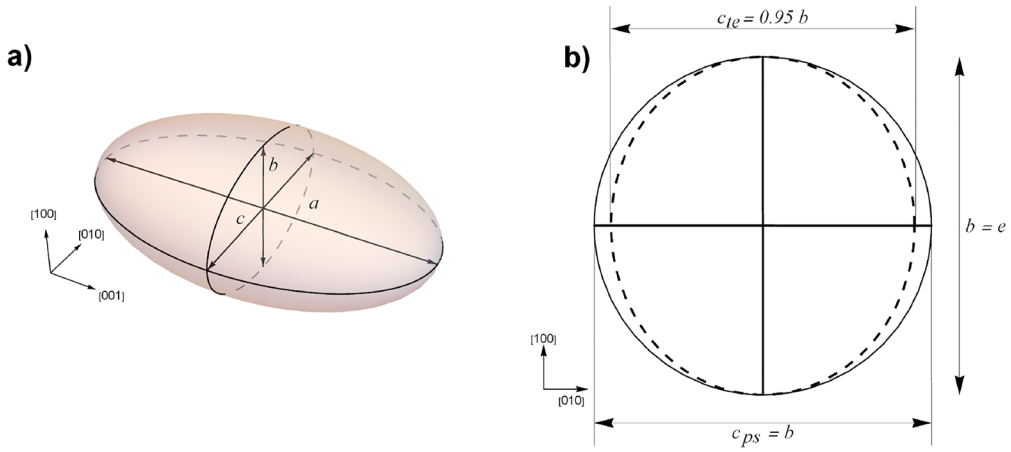

Figure 1. Particle geometry. (a) An ellipsoidal geometry with axes length a, b, and c. The spheroidal and triaxial ellipsoidal geometries used to describe the grain shapes investigated in this work are special cases based on this basic geometry. (b) Transversal view of the ellipsoidal shape depicted in (a). c_{ps}: minor axis width for prolate spheroids (which is equal in length to b); c_{te}: minor axis length for triaxial ellipsoids (=0.95 b); e: elongation (=b/a).

less than the exchange length l (Rave et al., 1998) to assure that exchange interactions are correctly accounted during the energy minimization:

$$l = \sqrt{\frac{2A}{\mu_0 M_s^2}}. \tag{1}$$

For taenite, l is ~3 nm. However, for smaller grain sizes an even finer mesh resolution was used: 1 nm for grains between 10 and 20 nm, 2 nm for grain sizes between 20 and 28 nm, and 3 nm for grain sizes >30 nm.

The domain structure that minimizes the grain's internal energy is referred to as a local energy minimum (LEM) state. We use the software Paraview (Ahrens et al., 2005) to visualize the magnetization structures associated to LEM states. To assess the magnetic stability of a particle, in principle all LEM states must be obtained. Although no computational method guarantees that all LEM states can be determined, by performing a large number of energy minimization seeded with initial random states for a given volume, it is possible to observe which LEM states are the most likely to occur. In this work, for each grain shape, 100 minimizations are performed. From the LEM states it is possible to estimate the stability of the magnetic state by calculating the energy barrier (ΔE) between any two different domain states. The nudge-elastic-band (NEB) method, implemented in MERRILL's micromagnetic routine, allows determination of the minimal energy path over which a transition between two distinct LEM states is likely to occur (Fabian & Shcherbakov, 2018). The energy barrier ΔE is then calculated as the difference between the maximum energy value along the minimal path determined by the NEB method and the energy of the initial LEM state. Based on ΔE the magnetic stability of a domain state is estimated by calculating the relaxation time associated with the transition using the Néel-Arrhenius equation (Néel, 1949):

$$\tau = \tau_0 \exp\left(\frac{\Delta E}{k_B T}\right), \tag{2}$$

with $\tau_0 = 10^{-9}$ s the atomic attempt time (Berndt et al., 2015), k_B the Boltzmann constant and T the temperature.

3. Results

3.1. Domain States in Nm-Sized Taenite

Micromagnetic results revealed a gradual change in taenite's domain state, from uniform to non-uniform, as a function of grain size. Both grain shapes (spheroidal and triaxial ellipsoidal) exhibit uniform single domain (SD) states magnetized along the long axis for smaller sizes (Figure 2 and Figure S3 in Supporting Information S1), while larger grains display non-uniform domain states. We observed three different non-SD structures: (a)

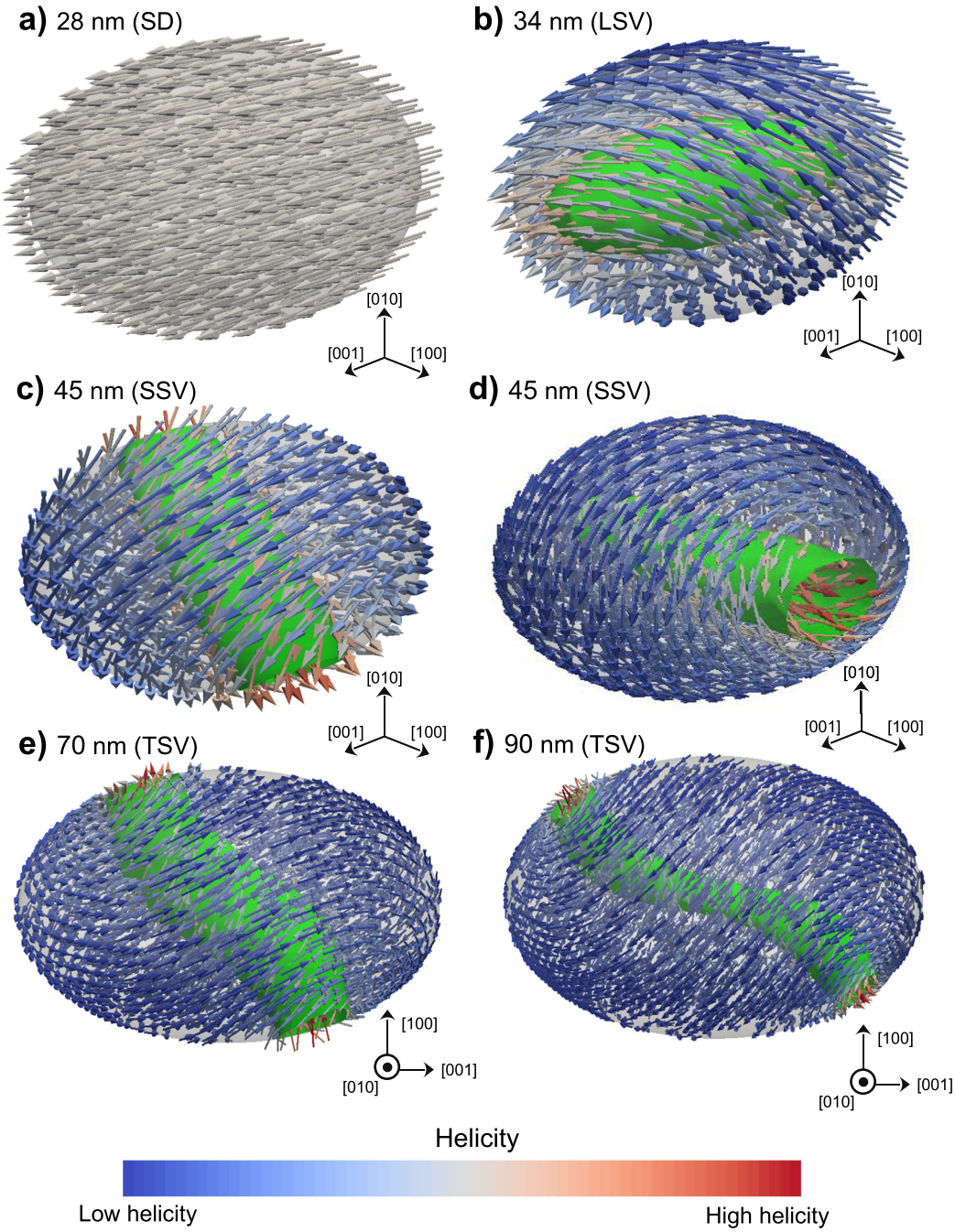

Figure 2. Magnetic domain structures for 30% elongated, spheroidal taenite grains with different sizes. (a) Single domain state (28 nm); (b) LSV state (34 nm); (c, d): two different SSV states observed in a 45 nm sized grain; (e) TSV state (70 nm); (f) TSV state (90 nm). The green surfaces are helicity iso-surfaces. The same domain states and size thresholds were observed in triaxial grains (see Table S1 in Supporting Information S1).

long-axis-aligned-SV (LSV), in which a magnetic vortex is aligned with the long axis of the grain (Figure 2b and Figure S1 in Supporting Information S1), (b) short-axis-aligned-SV (SSV), in which the vortex core is aligned with the short axis (Figures 2c and 2d) and (c) "twisted-SV" (TSV) states, in which the vortex core does not follow a straight line (Figures 2e and 2f). The latter is possibly a transitional state from a single vortex (SV) to a multi-vortex state.

The critical grain sizes that mark transitions between distinct domain structures were obtained from size hysteresis loops (Ó Conbhuí et al., 2018) (Figure S1 in Supporting Information S1). In size loops, small (10 nm sized) single domain (SD) taenite grains are gradually increased in size until they spontaneously switch to vortex states (upper branch). Once the maximum size (90 nm) is reached, the size of the grain is then scaled down until a SD state is reached again (lower branch). From size loops we extracted three critical size: from lower branches, the smallest grain sizes that can form non-SD indicates the transition uniform (SD) to non-uniform (LSV) domain states $\left(d_{LSV}^{\mathrm{SD}}\right)$. From upper branches we extracted the critical sizes at which LSV states transform into SSV ones $\left(d_{SSV}^{LSV}\right)$ and at which SSV are transform into TSV states $\left(d_{TSV}^{SSV}\right)$. We note that during grain shrinking (lower branches), transitions from TSV/SSV back to LSV states were observed at the same sizes observed in the upper branches. This sequence of domain states (SD to LSV to SSV to TSV) was observed in both spheroidal and triaxial grains, and the critical grain sizes were virtually identical (Table S4 in Supporting Information S1). However, grains in the SSV to TSV range show an important difference in behavior depending on the spheroidal/triaxial shape: while triaxial grains have four distinct stable domain states (each differing only in the sign of the total magnetic moment and the sign of the total vorticity), spheroidal grain's vortex cores (and therefore, magnetic moment vectors) are free to rotate about the elongation axis (SSV), or about a certain solid angle around the elongation axis (TSV) (Figure S3 in Supporting Information S1). This effect is due to the rotational symmetry of spheroidal grains, together with the extremely weak magnetocrystalline anisotropy of taenite.

3.2. Energy Barriers

NEB results indicate two mechanisms of magnetization reversal in the SD size range: (a) via coherent rotation (CR), in which the SD structure as a whole is rotated coherently, and (b) via vortex nucleation (VN), which involves the nucleation of a magnetic vortex through the minimized energy path (usually a SSV state, Figure 2d), rotation of the vortex structure, and reestablishment of a uniform state. CR is observed in grain sizes $\lesssim d_{LSV}^{\mathrm{SD}}$, while reversals via VN are observed in the proximity of the uniform to non-uniform transition (i.e., grains sizes $\sim d_{LSV}^{\mathrm{SD}}$). Energy barriers associated to CR reversals are larger than those that occur via VN (Figure 3a).

There are narrow transition zones in the proximity of d_{LSV}^{SD}, d_{SSV}^{LSV}, and d_{TSV}^{SSV} of around ∼4 to ∼12 nm, where more than one domain structure can occur (see Figure S1 in Supporting Information S1). For instance, in the proximity of d_{LSV}^{SD}, both SD (with higher internal energy) and LSV (with lower internal energy) states are observed within the micromagnetic solutions; in these cases, we used only the lowest energy domain states to calculate energy barriers. Transitions between LSV states of opposite magnetic moment (Figures 3e and 3k) occur through a process similar to CR, in which the whole vortex structure is rotated coherently (structure CR, Nagy et al. (2017)).

SSV and TSV states in spheroidal grains can occur in any direction about a solid angle, without any effective energy barrier between these different states. In triaxial grains, however, the small deformation about the intermediate axis is sufficient to create an energy barrier of a magnitude comparable or higher than that of LSV transitions (Figure 3 and Figure S3 in Supporting Information S1).

3.3. Domain State Stability

For spheroidal grains, superparamagnetic (SP) states (relaxation times <100 s) form below ∼14 nm. From ∼14 to ∼32 nm a sharp increase in relaxation time is observed, such that above ∼14 nm SD states are stable over geological timescales (Figure 4). SD states transitions via CR usually have larger energy barriers than those that occur via VN; this causes a decrease in relaxation times for sizes between ∼32 to ∼40 nm where VN magnetization reversals are observed. One should note, however, that the relaxation times within this range of sizes are still significantly high, indicating that SD taenite is always stable above ∼14 nm, regardless the mechanism of magnetization reversal. Up to the 40–50 nm (depending on elongation), particles adopt a LSVconfiguration. LSV–LSV transitions are less demanding energetically than those involving SD states (either by CR or VN), which further decreases the relaxation times within this size range. However, most relaxation times associated to LSV–LSV transition are still very high, indicating that LSV are most stable over solar system timescales. Above the LSV range, spheroidal particles become SSV/TSV, and hence have zero energy barrier, allowing them to freely rotate about a solid angle—their relaxation time therefore approaches zero. Triaxial grains, on the other hand (while showing the same behavior for small sizes), do not have this rotational symmetry: Therefore, the larger SSV/TSV grains (starting from 30 to 50 nm depending on elongation), have increasingly larger energy barriers, such

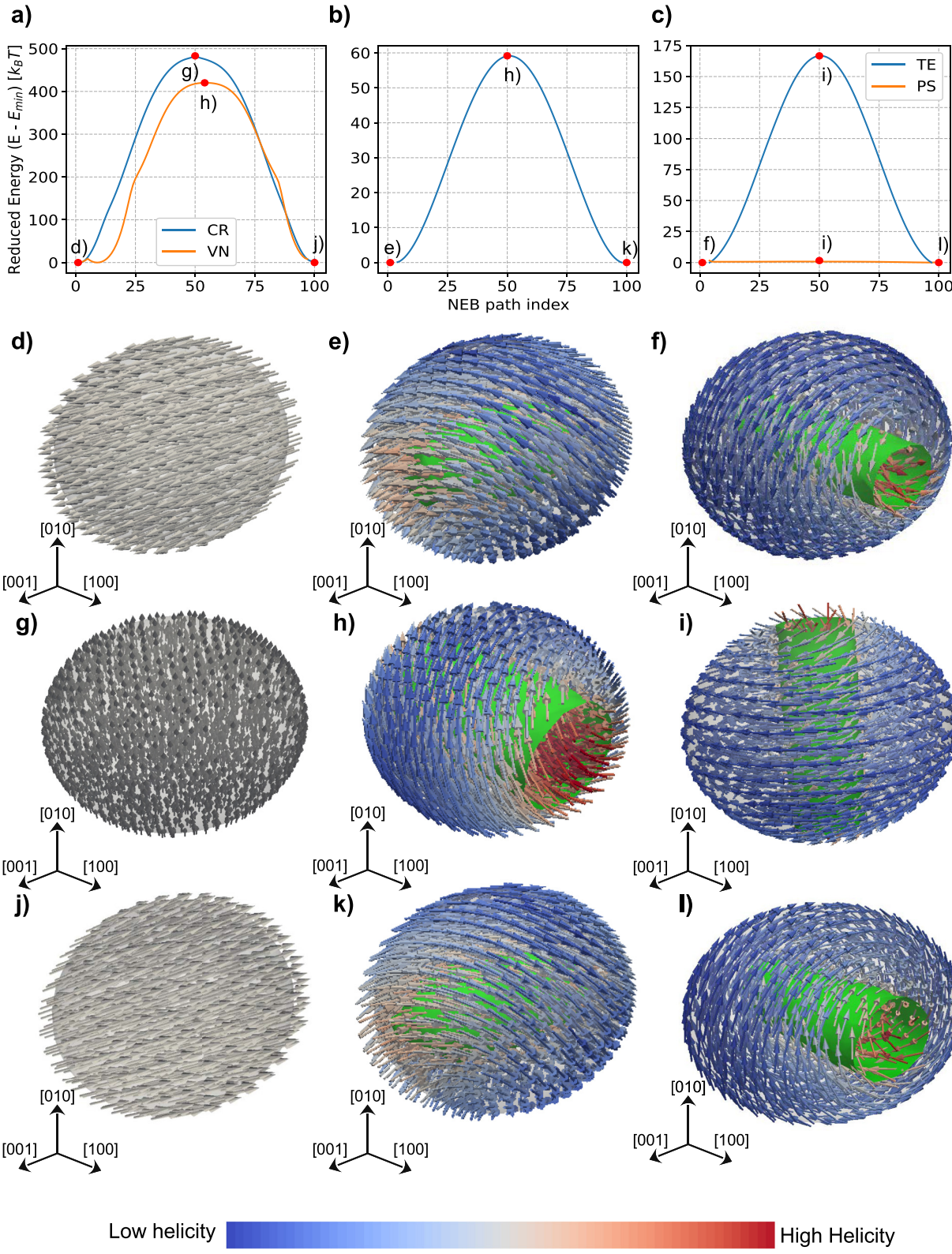

Figure 3. Transitions between different domain state in spheroidal taenite grains. (a–c) Energy barriers, (d–l) domain states of ground state, maximum energy state, and opposite ground state. Left column: SD−SD transition through coherent rotation (CR); center column: LSV–LSV transition; right column: SSV–SSV transition for a triaxial ellipsoid (TE, blue line) and a prolate spheroid (PS, orange line). Also in (a): some larger single domain states transition through vortex nucleation (VN, orange line), through a sequence given by Figures (d)–(h)–(j).

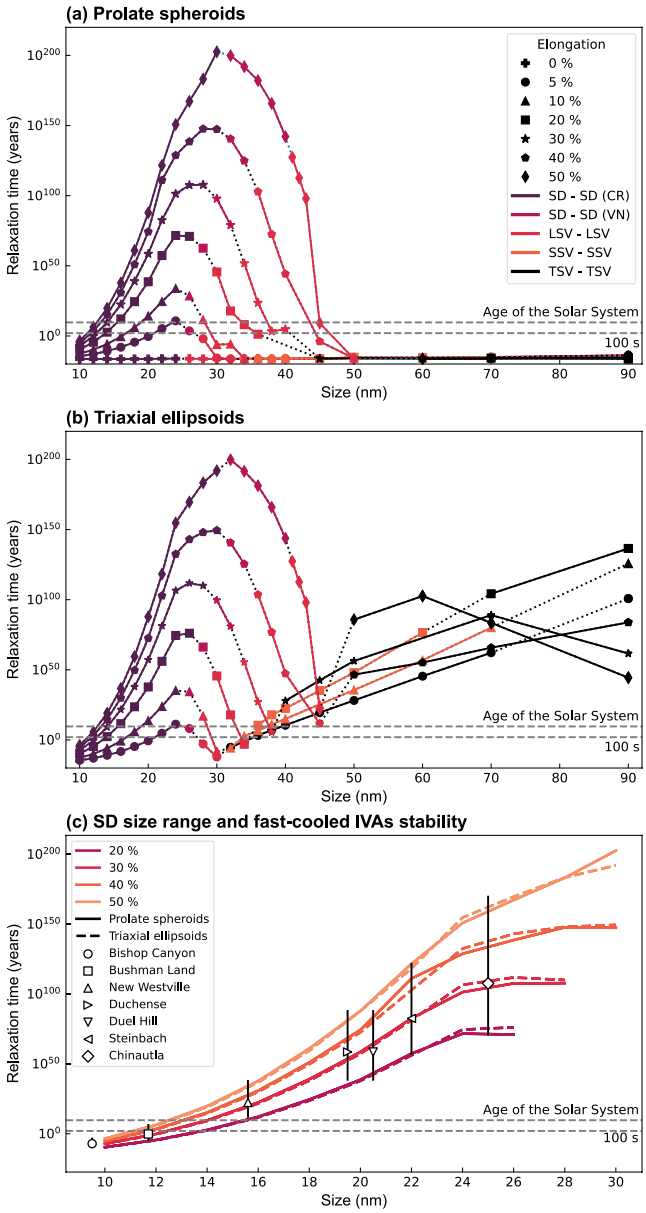

Figure 4. Relaxation times of (a) spheroidal, (b) triaxial taenite grains (between 10 and 90 nm) and (c) within the single domain size range for both shapes (<30 nm). In (a) and (b), symbols denote the elongation of the grain, while different colors correspond different domain state transitions (see inset in a). In (c), hollow symbols are the relaxation times calculated for island sizes of some IVA meteorites (Table S5 in Supporting Information S1). We consider particles with 78% of the island sizes observed experimentally, as this is suggested to be the approximate size of the islands at 320°C (Maurel et al., 2019). Lines correspond to the different elongations (in %). The bars correspond to the highest (50%) and lowest (20%) elongations, respectively, used to calculate the relaxation times for the IVAs.

that—apart from the narrow low-stability trough around 30–50 nm—particles become very stable again.

4. Discussion

4.1. Paleomagnetic Potential of Taenite-Containing Cloudy Zones

Micromagnetic results presented in this work indicate that taenite forms SV states in grain sizes $\gtrsim$34 nm (depending on elongation), which is in agreement with previous numerical models (Einsle et al., 2018). Our results also show, however, that there is a size range, from ~14 to ~34 nm, for which taenite forms stable SD states (Figure 4). The existence of a SD range in nm-sized taenite grains has important implications for different iron meteorite groups. Fast cooled IVAs (>150–2500°C/Myr) are believed to preserve fine-grained (<50 nm) CZs that contain (totally or partially) disordered taenite islands as a consequence of rapid cooling (and the different M-shaped Ni diffusion profile, Nichols et al. (2020)). This indicate that, contrarily to previously assumed, the low coercivity observed in bulk taenite does not imply low domain state stability (Bryson et al., 2017; Nichols et al., 2020). Nanometer-sized taenite can preserve stable magnetization states, making taenite-containing CZs good candidates to provide reliable paleomagnetic records of ancient dynamo activity in meteorites. Note that fast cooling for iron meteorites is still at sufficiently slow rates (see Table S4 in Supporting Information S1), that we can expect the change in temperature to be slower than the increase in grain size with respect to controlling the blocking of the grains' magnetization. Therefore, we suggest that fast cooled meteorites are able to preserve stable crystallization remanent magnetizations (CRMs) in their CZs over billion-year timescales. This opens the possibility of assessing ancient dynamo activity based on record preserved in taenite-containing CZs of fast cooled iron meteorites.

It is worth mentioning that in tightly-packed, coarsed-grained intermediate CZs, magnetostatic interactions are expected to play a significant role in the CZ's recording mechanism (Einsle et al., 2018; Mansbach et al., 2022). Recent works shown that interaction fields in small clusters of closed-packed tetrataenite grains can be of the order of ~275 mT, which is the same order of magnitude of the critical fields at which domain walls in multi-domain (MD) tetrataenite are destroyed and SD states are favored (Mansbach et al., 2022). On the other hand, interaction fields in clusters of (SV) taenite grains seems to not play a significant role, since the same (SV) domain states are observed in both individual grains as well as in clusters of interacting grains (Einsle et al., 2018). Moreover, recent numerical results indicate that CRMs are significantly less sensitive to magnetostatic interaction fields than thermomagnetic remanences recorded by the same grain size at higher temperatures (Baker & Muxworthy, 2023). It is reasonable to expected that these apply for taenite-containing CZs in fast cooled meteorites, since our results indicate that SD taenite blocks (i.e., records stable CRMs) at sizes as smaller as ~14 nm, that is, when interaction effects are significantly reduced due to the weak magnetic moment (and, thus, weak overall interaction field) of the grains. We suggest, therefore, that in taenite-containing CZs of fast cooled meteorites, magnetostatic interactions are likely to play a minor role, which indicates that grain/islands growth is solely the main factor in controlling blocking of stable paleomagnetic records in this microstructure. Therefore, our model provides a numerical estimate of the blocking volume (~14 nm, depending on elongation) at which stables records are created in taenite-containing CZs. Based on experimentally measured island sizes of IVA meteorites (C. Yang et al., 1997; Goldstein et al., 2009), our results indicate that most of them are likely to have

formed stable SD taenite grains at ≳320°C (Figure 4c). It shows that even in extreme cases when the rapid cooling of meteoritc material prevents tetrataenite from ordering, the precursor taenite is also capable of preserving stable magnetization states over billion-years timescales, thus providing reliable records of ancient dynamo fields.

One should note, however, that fast cooled meteorites may either avoid ordering to tetrataenite, or in some cases partially or completely order to tetrataenite (e.g., IVA Steinbach, Bryson, Herrero-Albillos, et al. (2014)). The ordering of tetrataenite has already been investigated using micromagnetic modeling, showing that SV states in ∼80 to ∼90 nm sized taenite islands undergo a series of domain modifications during tetrataenite ordering (implying that any remanence preserved by the precursor taenite is lost during the phase transition). Our results indicate, however, that in fast cooled IVAs, tetrataenite forms from underlying (and highly stable) SD states in its precursor taenite. It is still poorly understood how tetrataenite's ordering affect the islands' domain state within taenite SD range, but it is reasonable to expect that the underlying domain structure (by producing straight fields that act upon the nucleating phase domain state) may play an important role in the way the ordered tetrataenite is magnetizated. It has long been suggested that fine-grained tetrataenite might inherit the domain state of its precursor taenite (Wasilewski, 1988), similar to remanence inheritance/enhancement upon maghemitization (Ge et al., 2014). Based on cooling rates of the IVAs (see Table S4 in Supporting Information S1), preservation (i.e., inheritance) of SD states through tetrataenite ordering could translate to a temporal discrepancy of up to $\sim 10^5$ years on the timing of paleomagnetic record. The processes by which tetrataenite (via nucleation and growth within disordered taenite, Lewis et al. (2014)) and maghemite (via oxidation of magnetite from grain surface to core, Ge et al. (2014)) are created are, however, different. Different nucleation/transformation mechanisms may impact how nucleating/growing phases record magnetization states. The effect of nucleation and growth of ordered tetrataenite within disordered taenite still needs to be addressed (especially within taenite SD size range) as it can directly affect the timing of paleomagnetic record (in fact, small planetesimals usually have short-lived thermomagnetic activity, so time lapses of the order of $\sim 10^5$ years might encompasses completely distinct stages—onset and quiescence of a dynamo, for instance Bryson et al. (2017)—of their magnetic history). We note, however, that fast cooled meteorites have different M-shape diffusion profiles compared to slow cooled meteorites (Uehara et al., 2011). This means that the local Ni content even next to the taenite rim may not reach ∼40 wt.% Ni (like in slowly cooled meteorites) but be lower (as Ni does not have time to diffuse from kamacite to the surrounding taenite). As a consequence, the islands in these fast cooled meteorites may form at lower temperatures than 400°C. We can expect, therefore, that in the IVAs the ordering or tetratenite can occur at even smaller sizes. Our results show that taenite forms stable SD states at sizes as smaller as 14 nm. Hence, based on our results we can expect that tetrataenite ordering in most IVAs—and possibly in IVBs and in finer (<50 nm) regions of CZs in intermediate cooled meteorites—is likely to occur within taenite's SD size range. Therefore, the recording mechanism in these meteorites is likely different from the observed for coarsed-grained (SV taenite-containing) intermediate CZs (Einsle et al., 2018).

4.2. Paleomagnetic Potential of Coarsed-Grained Taenite

Our results indicate that large (>50 nm) taenite grain sizes are expected to adopt vortex states (i.e., LSV, SSV or TSV) that are also stable over geological timescales. We suggest, therefore, that coarsed-grained, non-SD taenite-containing meteoritic plessite and basaltic achondrites should also be considered potential sources of paleomagnetic records. We note, however, that recent numerical models suggests that SV states in isolated taenite grains can be significantly modified during tetrataenite ordering (Einsle et al., 2018). According to Einsle et al. (2018), there is no obvious relationship between the domain states (structure, intensity and orientation) of the islands before and after tetrataenite ordering, suggesting that any remanence possibly preserved by the precursor taenite is lost the ordering takes place. One can argue, however, that taenite is observed over a wider compositional range (Ni content from ∼10% to up to ∼50% (Uehara et al., 2011)), while tetrataenite forms in a narrower range (Ni content ∼50%). We can expect, therefore, that non-SD taenite grains are somehow common (or, at least, occur in a significant number) and, hence, are likely to carry a significant proportion of the total magnetic signal recorded by these microstructures. We reinforce, however, that understanding how non-SD states records magnetizations is a matter of intense research (Nagy et al., 2022). There is still the possibility of taenite and tetrataenite inclusions to coexist in the same microstructure (e.g., see Mansbach et al. (2022)), which would indicate that multiple records of ancient magentic activity can be recorded in the same sample: one event recorded by non-SD taenite at temperatures >400° to 320°C, and the other one recorded by (SD or MD, Mansbach et al. (2022)) at ≲320°C. Assessing these effects over the overall recorded magnetic signal in meteoritic plessite, despite their

relevance on meteoritic paleomagnetism, is beyond the scope of this work. Our results provides another numerical evidence that non-SD carriers (vastly observed in both terrestrial and extraterrestrial samples) can record stable magnetization states over billion-years timescales (Mansbach et al., 2022; Nagy et al., 2017, 2022; Shah et al., 2018; Valdez-Grijalva et al., 2018), which reinforce the potential of taenite-containing (stony-)iron meteorites in providing direct evidences of ancient thermal history of their parent bodies.

5. Conclusions

In this work we use finite-element 3D micromagnetic modeling to show that most nm-sized taenite grains observed in different microstructures preserved in meteorites can record stable magnetization states over billion-years timescales. Both SD (that form in the fine-grained CZs of fast cooled IVAs) as well as non-SD (that form in coarse-grained meteoritic plessite) states are able to provide reliable paleomagnetic records of ancient activity in meteorites. Our model provides a numerical estimate of the blocking volume of nm-sized SD taenite (∼14 nm, depending on elongation) in meteoritic CZs of fast cooled IVAs, and shows that in meteoritic plessite, paleomagnetic signals are dominated by non-SD taenite. Based on our results, we conclude that taenite-containing meteorite samples should be considered potential sources of paleomagnetic record, which thus provides a unique opportunity of investigating key aspect of core formation and dynamo generation based on magnetic records preserved in nm-sized taenite grains.

Data Availability Statement

All results reported here were generated using the open source micromagnetic modeling code MERRILL (Ó Conbhuí et al., 2018). A complete guide to installation and use of MERRILL is described here: https://blogs.ed.ac.uk/rockmag. The data required to reproduce our results (MERRILL script and geometries) is available at https://github.com/devienne/taenite_tetrataenite.

Acknowledgments
J.A.P.M.D. is funded by the Chinese Scholarship Council (CSC). J.A.P.M.D. and T.A.B. acknowledges funding from the Natural Sciences Foundation of China (NSFC) (Grant 42174082) and T.A.B acknowledges further NSFC funding (Grant 42150410384). W.W. acknowledges the Natural Environment Research Council (NERC) Grants (NE/V001388/1, NE/S011978/1, and NE/W006707/1). L.N. acknowledges the Natural Environment Research Council (NERC) (Grant NE/V014722/1). The authors are grateful to Dr. James Bryson (Univ. Oxford) for fruitful discussions. The authors would like to thank the anonymous reviewers for their valuable comments.

References

Ahrens, J., Geveci, B., & Law, C. (2005). Paraview: An end-user tool for large-data visualization. In *Visualization handbook*. Elsevier.

Baker, E. B., & Muxworthy, A. R. (2023). Using Preisach theory to evaluate chemical remanent magnetization and its behavior during thellier-thellier-coe paleointensity experiments. *Journal of Geophysical Research: Solid Earth*, *128*(2), e2022JB025858. https://doi.org/10.1029/2022JB025858

Berndt, T., Muxworthy, A. R., & Paterson, G. A. (2015). Determining the magnetic attempt time τ_0, its temperature dependence, and the grain size distribution from magnetic viscosity measurements. *Journal of Geophysical Research: Solid Earth*, *120*(11), 7322–7336. https://doi.org/10.1002/2015JB012283

Bryson, J. F., Church, N. S., Kasama, T., & Harrison, R. J. (2014). Nanomagnetic intergrowths in Fe-Ni meteoritic metal: The potential for time-resolved records of planetesimal dynamo fields. *Earth and Planetary Science Letters*, *388*, 237–248. https://doi.org/10.1016/j.epsl.2013.12.004

Bryson, J. F., Herrero-Albillos, J., Kronast, F., Ghidini, M., Redfern, S. A., Van der Laan, G., & Harrison, R. J. (2014). Nanopaleomagnetism of meteoritic Fe-Ni studied using x-ray photoemission electron microscopy. *Earth and Planetary Science Letters*, *396*, 125–133. https://doi.org/10.1016/j.epsl.2014.04.016

Bryson, J. F., Nichols, C. I., Herrero-Albillos, J., Kronast, F., Kasama, T., Alimadadi, H., et al. (2015). Long-lived magnetism from solidification-driven convection on the pallasite parent body. *Nature*, *517*(7535), 472–475. https://doi.org/10.1038/nature14114

Bryson, J. F., Weiss, B. P., Getzin, B., Abrahams, J. N., Nimmo, F., & Scholl, A. (2019). Paleomagnetic evidence for a partially differentiated ordinary chondrite parent asteroid. *Journal of Geophysical Research: Planets*, *124*(7), 1880–1898. https://doi.org/10.1029/2019JE005951

Bryson, J. F., Weiss, B. P., Harrison, R. J., Herrero-Albillos, J., & Kronast, F. (2017). Paleomagnetic evidence for dynamo activity driven by inward crystallisation of a metallic asteroid. *Earth and Planetary Science Letters*, *472*, 152–163. https://doi.org/10.1016/j.epsl.2017.05.026

Buchwald, V. F. (1975). *Handbook of iron meteorits*. University of California Press.

Einsle, J. F., Eggeman, A. S., Martineau, B. H., Saghi, Z., Collins, S. M., Blukis, R., et al. (2018). Nanomagnetic properties of the meteorite cloudy zone. *Proceedings of the National Academy of Sciences*, *115*(49), E11436–E11445. https://doi.org/10.1073/pnas.1809378115

Elkins-Tanton, L. T., Weiss, B. P., & Zuber, M. T. (2011). Chondrites as samples of differentiated planetesimals. *Earth and Planetary Science Letters*, *305*(1–2), 1–10. https://doi.org/10.1016/j.epsl.2011.03.010

Fabian, K., & Shcherbakov, V. P. (2018). Energy barriers in three-dimensional micromagnetic models and the physics of thermoviscous magnetization. *Geophysical Journal International*, *215*(1), 314–324. https://doi.org/10.1093/gji/ggy285

Ge, K., Williams, W., Liu, Q., & Yu, Y. (2014). Effects of the core-shell structure on the magnetic properties of partially oxidized magnetite grains: Experimental and micromagnetic investigations. *Geochemistry, Geophysics, Geosystems*, *15*(5), 2021–2038. https://doi.org/10.1002/2014GC005265

Gehrmann, B. (2005). Nickel–iron alloys with special soft magnetic properties for specific applications. *Journal of Magnetism and Magnetic Materials*, *4*(35), 290–291. https://doi.org/10.1002/chin.200535242

Goldstein, J. I., & Michael, J. R. (2006). The formation of plessite in meteoritic metal. *Meteoritics & Planetary Sciences*, *41*(4), 553–570. https://doi.org/10.1111/j.1945-5100.2006.tb00482.x

Goldstein, J. I., Scott, E. R., & Chabot, N. L. (2009). Iron meteorites: Crystallization, thermal history, parent bodies, and origin. *Chemie der Erde*, *69*(4), 293–325. https://doi.org/10.1016/j.chemer.2009.01.002

Hÿtch, M. J., Dunin-Borkowski, R. E., Scheinfein, M. R., Moulin, J., Duhamel, C., Mazaleyrat, F., & Champion, Y. (2003). Vortex flux channeling in magnetic nanoparticle chains. *Physical Review Letters*, *91*(25), 257207. https://doi.org/10.1103/PhysRevLett.91.257207

Lewis, L. H., Mubarok, A., Poirier, E., Bordeaux, N., Manchanda, P., Kashyap, A., et al. (2014). Inspired by nature: Investigating tetrataenite for permanent magnet applications. *Journal of Physics: Condensed Matter*, *26*(6), 064213. https://doi.org/10.1088/0953-8984/26/6/064213

Mansbach, E. N., Shah, J., Williams, W., Maurel, C., Bryson, J. F. J., & Weiss, B. P. (2022). Size ranges of magnetic domain states in tetrataenite. *Geochemistry, Geophysics, Geosystems*, *23*(11), e2022GC010631. https://doi.org/10.1029/2022GC010631

Maurel, C., Bryson, J. F. J., Lyons, R. J., Ball, M. R., Chopdekar, R. V., Scholl, A., et al. (2020). Meteorite evidence for partial differentiation and protracted accretion of planetesimals. *Science Advances*, *1*(30), 1–10. https://doi.org/10.1126/sciadv.aba1303

Maurel, C., Weiss, B. P., & Bryson, J. F. (2019). Meteorite cloudy zone formation as a quantitative indicator of paleomagnetic field intensities and cooling rates on planetesimals. *Earth and Planetary Science Letters*, *513*, 166–175. https://doi.org/10.1016/j.epsl.2019.02.027

McCoy, T., Mittlefehldt, D., & Wilson, L. (2006). Asteroid differentiation. In *Meteorites and the early solar system II* (pp. 733–745). Cambridge University Press.

Nagy, L., Williams, W., Muxworthy, A. R., Fabian, K., Almeida, T. P., Conbhuí, P. Ó., & Shcherbakov, V. P. (2017). Stability of equidimensional pseudo-single-domain magnetite over billion-year timescales. *Proceedings of the National Academy of Sciences*, *114*(39), 10356–10360. https://doi.org/10.1073/pnas.1708344114

Nagy, L., Williams, W., Tauxe, L., & Muxworthy, A. (2022). Chasing tails: Insights from micromagnetic modeling for thermomagnetic recording in non-uniform magnetic structures. *Geophysical Research Letters*, *49*(23), e2022GL101032. https://doi.org/10.1029/2022GL101032

Néel, L. (1949). Théorie du trainage magnétique des ferromagnétiques en grains fins avec application aux terres cuites. *Annales de Géeophysique*, 99–136.

Nichols, C. I., Bryson, J. F., Cottrell, R. D., Fu, R. R., Harrison, R. J., Herrero-Albillos, J., et al. (2021). A time-resolved paleomagnetic record of main group pallasites: Evidence for a large-cored, thin-mantled parent body. *Journal of Geophysical Research: Planets*, *126*(7), e2021JE006900. https://doi.org/10.1029/2021JE006900

Nichols, C. I., Bryson, J. F., Herrero-Albillos, J., Kronast, F., Nimmo, F., & Harrison, R. J. (2016). Pallasite paleomagnetism: Quiescence of a core dynamo. *Earth and Planetary Science Letters*, *441*, 103–112. https://doi.org/10.1016/j.epsl.2016.02.037

Nichols, C. I., Bryson, J. F. J., Blukis, R., Herrero-Albillos, J., Kronast, F., Rüffer, R., et al. (2020). Variations in the magnetic properties of meteoritic cloudy zone. *Geochemistry, Geophysics, Geosystems*, *21*(2), e2019GC008798. https://doi.org/10.1029/2019GC008798

Nichols, C. I., Krakow, R., Herrero-Albillos, J., Kronast, F., Northwood-Smith, G., & Harrison, R. J. (2018). Microstructural and paleomagnetic insight into the cooling history of the IAB parent body. *Geochimica et Cosmochimica Acta*, *229*, 1–19. https://doi.org/10.1016/j.gca.2018.03.009

Ó Conbhuí, P., Williams, W., Fabian, K., Ridley, P., Nagy, L., & Muxworthy, A. R. (2018). MERRILL: Micromagnetic Earth related robust interpreted language laboratory. *Geochemistry, Geophysics, Geosystems*, *19*(4), 1080–1106. https://doi.org/10.1002/2017GC007279

Rave, W., Fabian, K., & Hubert, A. (1998). Magnetic states of small cubic particles with uniaxial anisotropy. *Journal of Magnetism and Magnetic Materials*, *190*(3), 332–348. https://doi.org/10.1016/S0304-8853(98)00328-X

Shah, J., Williams, W., Almeida, T. P., Nagy, L., Muxworthy, A. R., Kovács, A., et al. (2018). The oldest magnetic record in our solar system identified using nanometric imaging and numerical modeling. *Nature Communications*, *9*(1), 1173. https://doi.org/10.1038/s41467-018-03613-1

Uehara, M., Gattacceca, J., Leroux, H., Jacob, D., & Van Der Beek, C. J. (2011). Magnetic microstructures of metal grains in equilibrated ordinary chondrites and implications for paleomagnetism of meteorites. *Earth and Planetary Science Letters*, *306*(3–4), 241–252. https://doi.org/10.1016/j.epsl.2011.04.008

Valdez-Grijalva, M. A., Nagy, L., Muxworthy, A. R., Williams, W., & Fabian, K. (2018). The magnetic structure and palaeomagnetic recording fidelity of sub-micron greigite (Fe_3S_4). *Earth and Planetary Science Letters*, *483*, 76–89. https://doi.org/10.1016/j.epsl.2017.12.015

Wasilewski, P. (1988). Magnetic characterization of the new magnetic mineral tetrataenite and its contrast with isochemical taenite. *Physics of the Earth and Planetary Interiors*, *52*(1–2), 150–158. https://doi.org/10.1016/0031-9201(88)90063-5

Wright, Y., & Grady, M. M. (2006). Types of extraterrestrial material available for study. In *Meteorites and the early solar system II* (pp. 3–18). Cambridge University Press.

Yang, C., Williams, D., & Goldstein, J. (1997). Low-temperature phase decomposition in metal from iron, stony-iron, and stony meteorites. *Geochimica et Cosmochimica Acta*, *61*(14), 2943–2956. https://doi.org/10.1016/S0016-7037(97)00132-4

Yang, J., Goldstein, J. I., Michael, J. R., Kotula, P. G., & Scott, E. R. (2010). Thermal history and origin of the IVB iron meteorites and their parent body. *Geochimica et Cosmochimica Acta*, *74*(15), 4493–4506. https://doi.org/10.1016/j.gca.2010.04.011